Article

Calculation of p*K* Values of Nucleobases and the Guanine Oxidation Products Guanidinohydantoin and Spiroiminodihydantoin using Density Functional Theory and a Polarizable Continuum Model

Vincenzo Verdolino, Roberto Cammi, Barbara H. Munk, and H. Bernhard Schlegel

More About This Article

Additional resources and features associated with this article are available within the HTML version:

- Supporting Information
- Access to high resolution figures
- Links to articles and content related to this article
- Copyright permission to reproduce figures and/or text from this article

View the Full Text HTML

ACS Publications
High quality. High impact.

Calculation of pK_a Values of Nucleobases and the Guanine Oxidation Products Guanidinohydantoin and Spiroiminodihydantoin using Density Functional Theory and a Polarizable Continuum Model

Vincenzo Verdolino,[†] Roberto Cammi,[†] Barbara H. Munk,[‡] and H. Bernhard Schlegel*,[‡]

Department o di Chimica Generale ed Inorganica, Università di Parma, Parco Area della Scienze 1, 43100 Parma, Italy and Department of Chemistry, Wayne State University, Detroit, Michigan, 48202

An efficient computational method has been identified that uses B3LYP density functional theory, IEF-PCM solvation modeling with a modified UFF cavity, and Boltzmann weighting of tautomers to predict the site-specific and global pK_a of DNA nucleobases and their oxidation products. The method has been used to evaluate the acidity of guanidinohydantoin (Gh) and spiroiminodihydantoin (Sp), two highly mutagenic guanine oxidation products. The trend observed for the pK_a values of Gh (9.64 and 8.15) is consistent with the experimentally observed values for guanidine cation (13.7) and hydantoin (9.16). The pK_{a1}(calc) value for deprotonation of Sp cation (Sp$^+$ → Sp) is very close to the experimentally observed pK_{a1} for 8-oxoG and is consistent with the similarity in their structures. The data suggest that the imide (N7) proton in Sp is considerably more acidic than that in Gh, possibly due to the presence of the through-space electronic effects of the carbonyl group located at C6. This difference in the acidity of Gh and Sp may be an indication of their potential toxicity and mutagenicity in vivo and remains a fertile area for experimental study.

1. Introduction

Damage to DNA via oxidation is thought to be related to a variety of cancers and neurological disorders as well as cell aging and death.[1−5] Typical damage involves chemical oxidation of the nucleobases or the pentose sugars, base cleavage, or the formation of DNA/protein cross-links. Oxidation of the guanine base leads to a variety of products including 8-oxo-7,8-dihydro-2′-deoxyguanine (8-oxoG), guanidinohydantoin (Gh), and spiroiminodihydantoin (Sp).[6−8] Gh and Sp are two of the major products observed in guanine oxidation and are thought to be formed via a common intermediate, 5-hydroxy-8-oxo-7,8-dihydroguanosine, with the product branching ratio dependent on the pH of the reaction environment.[9−13] Computational studies conducted by our group[14] confirmed that protonation or deprotonation of various sites within the intermediate species involved in the mechanism of formation of Gh and Sp had a significant effect on the predicted kinetics and thermodynamics of the various pathways. For future studies of acid- or base-catalyzed chemical reactions, it would be useful to have an efficient computational method to predict the site-specific protonation state or pK_a of intermediate species at experimental reaction pHs.

In addition to understanding the likely mechanisms for pH-sensitive reactions, a theoretical method for computing relative pK_as might prove useful for predicting the relative toxicity or mutagenicity of these adducts. The structural and functional changes observed in DNA following oxidation of its nucleobases may be due, in part, to changes in the hydrogen-bonding characteristics of the oxidized adducts. Hydrogen bonding between the nucleobases in DNA and RNA duplexes is known to be very important to their structure and function in vivo.[15]

The strength of these hydrogen bonds is correlated to the relative pK_a values of the donor and acceptor nucleobases.[16] For several decades, research groups have used a variety of experimental techniques to measure the pK_a of the isolated DNA and RNA nucleobases as well as those attached to the ribose, deoxyribose, and the phosphate backbone.[8,17−22] The pK_a of nucleobases has been demonstrated to fluctuate depending on its location in the base sequence in the backbone of DNA and RNA,[18] its proximity to metal ions,[21] and its oxidation state.[8,19,20] Research groups have used computational methods to predict either the pK_a or protonation state of both modified[23,24] and unmodified nucleobases,[25−31] nucleotides,[32] and the guanine oxidation product, 8-oxoguanine.[33] The latter compound can be further oxidized in vivo to form Gh and Sp, two highly mutagenic DNA lesions.[34−37] In UV melting studies, both Gh and Sp were shown to decrease the thermodynamic stability of duplex DNA relative to guanine and 8-oxoguanine, with the effect of the Sp being more severe.[34,38] Molecular dynamics simulations indicate that Sp lesions alter the base stacking and Watson−Crick hydrogen-bonding interactions of the duplexes.[39,40] Although steric differences between the planar guanine and 8-oxoguanine and the nonplanar Gh and Sp compounds could certainly contribute to these conformational changes, it is also possible that the duplex destabilization is due, at least in part, to changes in the site specific pK_a values of these lesions relative to their parent compounds guanine and 8-oxoguanine.

The prediction of accurate pK_a values using computational techniques has been the subject of study for many years.[16,41−63] It is particularly challenging due to the fact that an error of 1.36 kcal/mol in the free energy calculation results in a error of 1 pK_a unit. A variety of computational methods have been used to study the relative acidity and basicity of the nucleobases and nucleosides.

Theoretical studies of the gas phase acidity of the isolated nucleobases were conducted by several groups. Giese and

* To whom correspondence should be addressed. Phone: (313) 577-2562; fax: (313) 577-8822; e-mail: hbs@chem.wayne.edu.
† Università di Parma.
‡ Wayne State University.

pKa Values of Nucleobases and Guanine Products

J. Phys. Chem. B, Vol. 112, No. 51, 2008 **16861**

SCHEME 1: Thermodynamic cycle used in the calculation of the pKa[a]
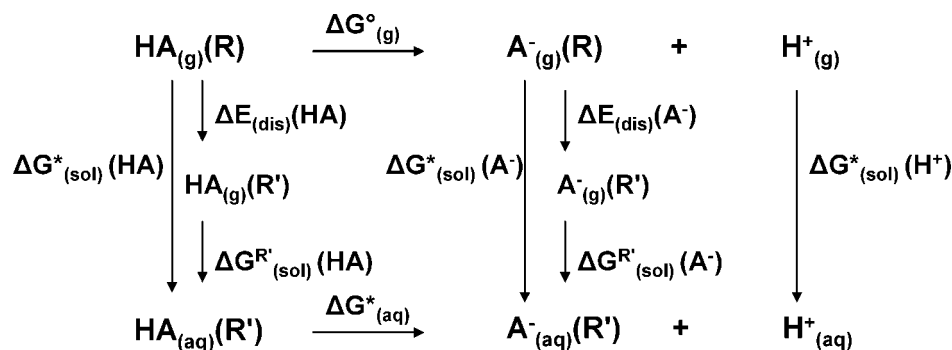
[a] The standard state reference for the gas phase free energy, $\Delta G^{\circ}_{(g)}$, is one atmosphere of pressure and 298.15 K, and for the free energy in water, $\Delta G^{*}_{(aq)}$, and free energy of solvation, $\Delta G^{*}_{(sol)}$, it is 1 M and 298.15 K. R is the structure optimized in the gas phase at B3LYP/6-31+G(d,p) and R′ is the structure optimized in solution at IEF-PCM/B3LYP/6-31+G(d,p). $\Delta E_{(dis)}$ is the electronic distortion energy between the gas and solution phase optimized structures calculated at the same level of theory with the aug-cc-pVTZ basis set. $\Delta G^{R'}_{(Sol)}$ is the calculated free energy of solvation of the R′ structure.

McNaughton studied the site-specific proton affinities of guanine and its heptahydrate at the B3LYP/6–31++G(d,p) level of theory. The proton affinity was calculated to be 229.7 kcal/mol and found to be consistent with the experimental value of 227.3 ± 11.5 kcal/mol.[31] Leszczynski calculated the proton affinities of the five nucleobases and the rare tautomers of guanine, adenine, and cytosine at the MP4(SDTQ)/6–31+G(d,p)//MP2/6–31+G(d,p) and MP2/6–311++G(d,p)//MP2/6–31+G(d,p) levels of theory. The calculated values were reported to be within 2.1% of the experimental values, and their data suggested that the rare tautomers of the nucleobases were a significant portion of the gas-phase equilibrium composition.[30] Chandra and Zeegers-Huyskens used B3LYP density functional theory and the 6–31++G(d,p) and 6–311++G(d,p) basis sets[26–29] to calculate the relative acidity of various tautomers of cytosine, thymine, and uracil, both alone and complexed with one molecule of water. They reported the relative acidities of the five nucleobases as uracil > thymine > guanine > adenine > cytosine.

The solution-phase pKa values of nucleotides in RNA have been calculated to within 1–2 pKa units using a modified version of the multiconformational continuum electostatics (MCCE) program that employs a variation of the Poisson–Boltzmann equation coupled with Monte Carlo treatment of the multiple ionization states.[32] This group predicted that significant shifts in the pKa of the adenine and cytosine nucleotides could be brought about by changes in the 3D structure of the RNA backbone and may be responsible for its function. Chatterjee et al.[22] estimated the effect of modification of the pentose-sugar on the site-specific pKa values for adenosine, guanosine, cytidine, thymidine, and uridine nucleosides using the closed-shell Hartree–Fock (HF) level of theory with a 6–31G(d,p) basis set. The conductor-like polarizable continuum model (CPCM) was used to calculate the free energy of solvation for each of the modified nucleosides, and the results were compared to experimental data. For these calculations, the free energy of solvation for the proton was assumed to be −263.47 kcal/mol. The authors reported a good linear correlation [R = 0.98, pKa(exp) = 0.4690(±0.0170) × pKa(calc) − 2.1087(±0.3270)] between the predicted pKa values of the nucleosides and the experimental values obtained with their corresponding bis-ethylphosphate nucleotides.

Using the B3LYP density functional theory and the Poisson–Boltzmann continuum-solvation model with modified atomic radii, Goddard's group has calculated both the site specific and overall pKa values of guanine, cytosine, isoguanine, 9-methyl-isoguanine, xanthine, and 8-oxoguanine.[23,25,33] By treating the solvation free energy of the proton as a variable ($\Delta G_{sol}(H^+)$ = −263.47 kcal/mol), they were able to predict the pKa of guanine within 0.2 units of experiment and the values for cytosine, isoguanine, xanthine, and 9-methylisoguanine within 1 unit of experiment. Goddard also estimated the relative abundance of deprotonated guanine at physiologic pH and discussed the role of the deprotonated species in base-pair mismatching during DNA replication. Using the same method, Hwang and Jang[24,64] predicted the pKa values of 9-methylguanine, 9-methyladenine, and 9-methylhypoxanthine to within 0.6–1.5 units of the experimental data. In this paper, we propose an efficient computational method for calculating the pKa of DNA and RNA nucleobases and the guanine oxidation products, Gh and Sp, employing the thermodynamic cycle outlined in Scheme 1, Boltzmann weighting of relevant tautomers, and modification of the UFF solvation cavity. The thermodynamic cycle is a modification of the one proposed by Nasimento et al.[59] for the calculation of absolute pKa values for carboxylic acids.

2. Computational Methods

General Formulas for Calculation of Global and Site-specific pKa Values. As noted in work previously published by Goddard's group,[25,33] the calculation of pKa values is complicated by the presence of multiple tautomers having various site-specific pKa values. We have followed the method outlined by Goddard for calculating a global pKa value from a Boltzmann weighting of the site-specific values of the various tautomers investigated in our study (eq 1). Where pK_a^{ij} is the site-specific value for deprotonation of tautomer i resulting in the formation of the deprotonated tautomer j, and f_i and f_j are the Boltzmann weighted fractions of tautomers i and j, respectively.

$$pK_a = pK_a^{ij} - \log f_i + \log f'_j \qquad (1)$$

The site-specific pKa of an acid HA is given by eq 2,

$$pK_a = \frac{1}{2.303RT}\Delta G^{*}_{(aq)} \qquad (2)$$

where R is the gas constant, T is the temperature, and $\Delta G^{*}_{(aq)}$ is the free energy of the deprotonation reaction, HA → H⁺ + A⁻,

for a standard state of 1 mol/L and room temperature. Using the thermocycle defined in Scheme 1, $\Delta G^*_{(aq)}$ is defined as the difference in the free energies in solution between the proton (H$^+$) and unprotonated tautomer (A$^-$) and the protonated tautomer (HA) (eq 3).

$$\Delta G^*_{(aq)} = G^*_{(aq)}(A^-_{R'}) + G^*_{(aq)}(H^+) - G^*_{(aq)}(HA_{R'}) \quad (3)$$

For each species, $G^*_{(aq)}$ is the sum of the gas phase standard free energy, $G^*_{(g)}$ and the free energy of solvation in water, $\Delta G^*_{(sol)}$, where the "*" indicates that all terms are in the standard state of 1 mol/L. To convert the calculated gas phase standard free energy, $G^\circ_{(g)}$, from its standard state of 1 atm gas phase/1 M solution to $G^*_{(g)}$ with a standard state of 1 M gas/1 M solution phase, it is necessary to add 1.89 kcal/mol ($RT \ln(1/R_gT)$),[65] (eq 4)

$$G^*_{(aq)} = G^*_{(g)} + \Delta G^*_{(sol)} = (G^\circ_{(g)} + 1.89) + \Delta G^*_{(sol)} \quad (4)$$

where R is 1.987 cal/mol·K and R_g is 8.206 × 10^{-2} liter·atm/mol·K. Combining equations 2, 3, and 4 yields a general expression for the calculation of the site-specific pK_a of a given tautomer (eqs 5.1–5.3).

$$pK_a = \frac{1}{2.303RT}(G^\circ_{(g)}(A^-) + 1.89 + \Delta G^*_{(sol)}(A^-) + G^\circ_{(g)}(H^+) + 1.89 + \Delta G^*_{(sol)}(H^+) - G^\circ_{(g)}(HA) - 1.89 - \Delta G^*_{(sol)}(HA)) \quad (5.1)$$

$$= \frac{1}{2.303RT}(G^\circ_{(g)}(A^-) + \Delta G^*_{(sol)}(A^-) + G^\circ_{(g)}(H^+) + 1.89 + \Delta G^*_{(sol)}(H^+) - G^\circ_{(g)}(HA) - \Delta G^*_{(sol)}(HA)) \quad (5.2)$$

$$= \frac{1}{2.303RT}(G^\circ_{(g)}(A^-) + \Delta G^*_{(sol)}(A^-) + G^\circ_{(g)}(HA) - \Delta G^*_{(sol)}(HA) - 270.29) \quad (5.3)$$

The gas and solution phase free energies of the proton were taken from the literature to be $G^\circ_{(g)} = -6.28$ kcal/mol[41] and $\Delta G^*_{(sol)} = -265.9$ kcal/mol,[65] respectively.

Calculation of Gas and Solution Phase Free Energies. Molecular orbital calculations were carried out using the E05 development version of the GAUSSIAN series of programs (Note: the PCM parameters change significantly between versions E05 and F01).[66] Optimized geometries and energies in the gas phase and in aqueous solution were computed with the B3LYP density functional method[67–69] using the 6−31+G-

SCHEME 2: Major tautomers and experimental pK_a values of guanine, 8-oxoguanine, adenine, thymine, and cytosine, evaluated for this study

pKa Values of Nucleobases and Guanine Products
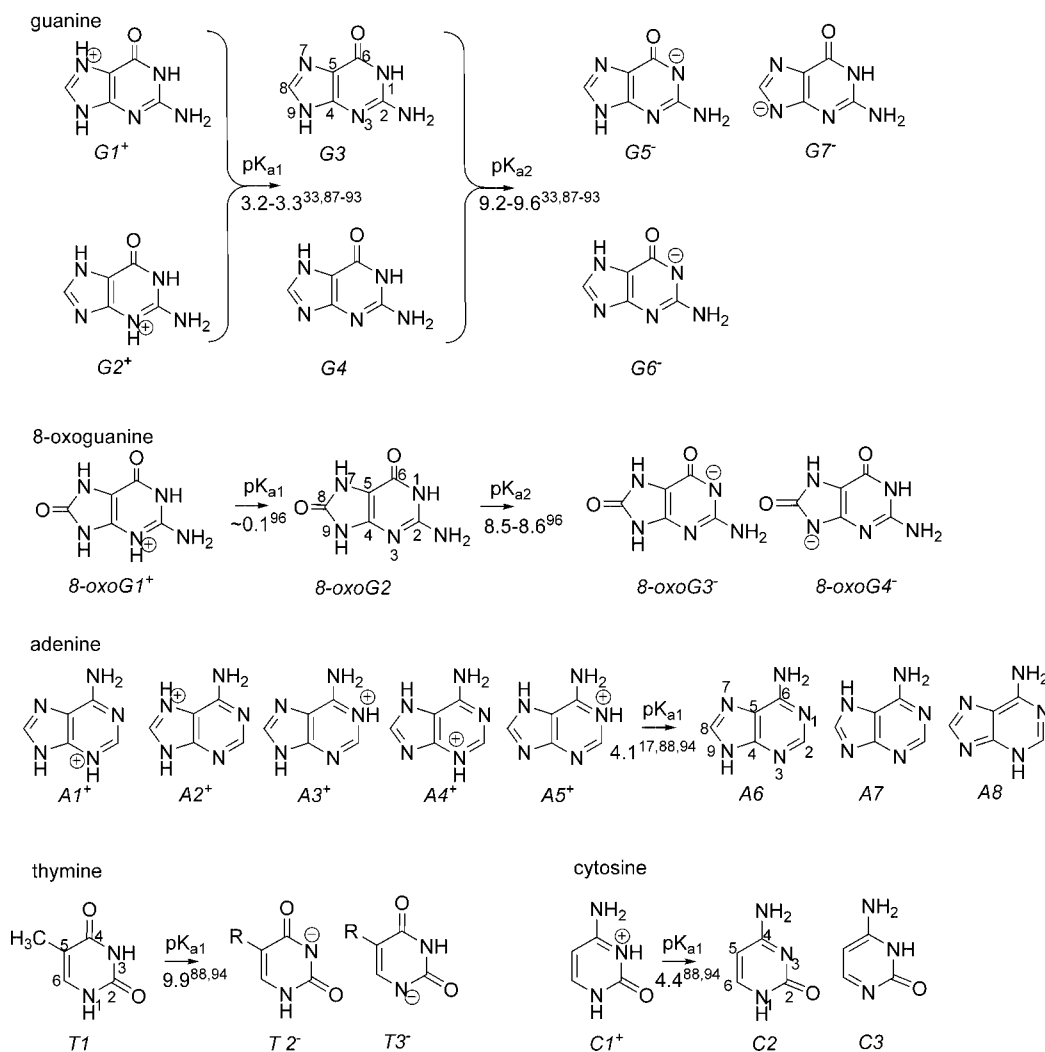
J. Phys. Chem. B, Vol. 112, No. 51, 2008 **16863**

TABLE 1: Relative Free Energies (kcal/mol), Calculated and Experimental pKa Values for Major Tautomers of Guanine, Adenine, Cytosine, Thymine, 8-oxoguanine, Hydantoin, Phenytoin, Guanidine, N-formylguanidine, and N-acetylguanidine

system	$\Delta G_{(g)}{}^a$ (kcal/mol)	$\Delta G^*_{(aq)}{}^a$ (kcal/mol)	$\Delta G^{R'}_{(sol)}{}^a$ (kcal/mol)	pK_a (calc)	pK_a (exp)
Guanine					
G1$^+$	0.0	0.0	−64.8		
G2$^+$	4.3	0.6	−68.9	3.4	3.2–3.3[b]
G3	0.3	1.5	−18.5		
G4	0.0	0.0	−19.0		
G5$^-$	2.8	0.0	−75.4	9.6	9.2–9.6[b]
G6$^-$	0.0	0.3	−72.0		
G7$^-$	0.8	0.7	−73.1		
Adenine					
A1$^+$	1.7	1.5	−60.4		
A2$^+$	8.0	2.8	−65.6		
A3$^+$	0.5	0.0	−60.7		
A4$^+$	0.0	0.3	−59.9	4.2	4.1[c]
A5$^+$	10.1	1.0	−69.5		
A6	0.0	0.0	−9.9		
A7	8.5	2.0	−16.7		
A8	8.5	4.5	−14		
Thymine					
T1	0.0	0.0	−11.1		
T2$^-$	0.0	0.6	−60.3	10.5	9.9[c]
T3$^-$	10.8	0.0	−72.3		
Cytosine					
C1$^+$	0.1	0.0	−65.8		
C2	0.0	0.0	−17.8	4.2	4.4[c]
C3	6.8	3.9	−21.0		
8-oxoG					
8-oxoG1$^+$	7.0	0.0	−82.6	−0.4	−0.1[d]
8-oxoG2	0.0	0.0	−21.0		
8-oxoG3$^-$	0.0	2.0	−69.6	8.0	8.5–8.6[d]
8-oxoG4$^-$	6.8	0.0	−79.1		
Hydantoin					
N1 anion	4.6	6.1	−69.9	11.0	9.16[e]
N3 anion	0.0	0.0	−67.9		
Phenytoin					
N1 anion	4.2	6.3	−54.1	8.7	8.31[e]
N3 anion	0.0	0.0	−55.8		
Guanidine	0.0	0.0	−62.5	14.5	13.7[f]
N-formyl guanidine					
FG1$^+$	0.0	0.0	−67.0	6.7	not available
FG2$^+$	7.6	3.3	−71.7		
FG3	0.0	0.0	−12.2		
FG8	8.1	0.8	−21.3		
N-acetyl guanidine					
AG1$^+$	0.0	0.0	−61.6	8.5	8.32[g]
AG2$^+$	11	7.5	−67.0		
AG3a	0.0	0.0	−9.78		
AG3b	0.1	0.1	−9.78		
AG5	2.0	2.8	−8.54		

[a] Energies were calculated using B3LYP density functional theory and the 6−31+G(d,p) and aug-cc-pVTZ basis sets. See eqs 4, 6, 13, 14, and 15. *[b]* References 25, 87−93. *[c]* Reference 88. *[d]* Reference 96. *[e]* Reference 103. *[f]* Reference 102. *[g]* Reference 108.

(d,p) basis set[70−75] (BS-I) with the latter calculations also employing integral equation formalism of the polarizable continuum model (IEF-PCM).[76−78] Tight convergence criteria and the "nosymm" options were used for all optimizations. The solution phase optimizations employed a solvent-excluding surface cavity model,[79] UFF radii,[80] and tesserae with an average area of 0.200 Å^2. For this study, all Gh and Sp chiral tautomers were the *R* stereoisomer. Given the symmetric nature of the PCM solvation model, it is antici-

pated that the calculated pKa values would be the same for the *S* isomer. Single-point calculations (in the gas phase) were also conducted with the gas phase and solution phase optimized geometries with the aug-cc-pVTZ[81] basis set (BS-II) and tight convergence criteria. Cartesian coordinates for the optimized geometries and electronic energies for all compounds are provided in the Supporting Information. Vibrational frequencies were computed in the gas phase at the B3LYP level with the 6−31+G(d,p) basis set (BS-I) and were used without scaling since the B3LYP frequencies agree quite well with experimental values for a wide range of second and third period compounds.[82] Thermal corrections and free energies were calculated by standard statistical thermodynamic methods[83] using the unscaled B3LYP frequencies and the ideal gas/rigid rotor/harmonic oscillator approximations. To improve the accuracy of the pKa calculated values versus experimental data, the solution phase single point calculation of the free energy of solvation employed a modified UFF cavity using an α value of 0.91 for the cationic and neutral species and 0.83 for the anionic species. Selection of the optimal α values was made by the empirical fitting process described below.

Calculation of pKa. Following optimization of each of the species in the gas phase, the standard gas phase free energy, $G^\circ_{(g)}$, for each species was calculated as the sum of the electronic energy at 0 K, the unscaled zero point energy, and the change in the free energy from 0 to 298 K (eq 6). Here R refers to the gas phase optimized structure.

$$G^\circ_{(g)}(R) = E^{B3LYP/aug-cc-pVTZ}_{(0\ K)}(R) + ZPE^{B3LYP/6-31+G(d,p)}(R) + \Delta G^{B3LYP/6-31+G(d,p)}_{(0\to298\ K)}(R) \quad (6)$$

The standard free energy of solvation in water $\Delta G^*_{(sol)}$, as described by Ben-Naim et al.,[84] is defined as the difference between the gas phase free energy at the gas phase optimized geometry, R, and the solution phase free energy at the solution phase optimized geometry, R′ (eqs 7 and 8).

$$\Delta G^*_{(sol)}(A^-) = G^*_{(aq)}(A^-_{R'}) - G^*_{(g)}(A^-_R) \quad (7)$$

$$\Delta G^*_{(sol)}(HA) = G^*_{(aq)}(HA_{R'}) - G^*_{(g)}(HA_R) \quad (8)$$

In the thermodynamic cycle outlined in Scheme 1, the standard free energy of solvation, $\Delta G^*_{(sol)}$, is partitioned into two physically meaningful parts (eqs 9 and 10): a deformation term that captures the electronic distortion energy resulting from the change in the geometry of the solute as the species moves from the gas phase (R) to the solution phase (R′), $\Delta E_{(dis)}$ (eqs 11 and 12), and a free energy of solvation term for the molecule at its geometry optimized in solution, $\Delta G^{R'}_{(sol)}$ (eqs 13 and 14). $\Delta G^{R'}_{(sol)}$ was obtained from a single-point calculation at the IEF-PCM/B3LYP/6−31+G(d,p) level of theory using the modified UFF cavity. The distortion energy ($\Delta E_{(dis)}$) for each species was computed from single-point calculations conducted at the B3LYP/aug-cc-pVTZ level of theory on the gas phase (R) and solution phase optimized (R′) structures optimized at B3LYP/6−31+G(d,p) and IEF-PCM/B3LYP/6−31+G(d,p) respectively.

$$\Delta G^*_{(sol)}(A^-) = \Delta G^{R'}_{(sol)}(A^-) + \Delta E_{(dis)}(A^-) \quad (9)$$

TABLE 2: Relative Free Energies (kcal/mol) and Population of Neutral Tautomers of Gh

	Gh1	Gh2	Gh3	Gh4	Gh5	Gh6	Gh7	Gh8	Gh9
gas phase									
$\Delta G_{(g)rel}^{\circ}$ [a]	6.4	0.0	27.6	24.2	20.9	21.7	23.4	17.5	25.9
population	1.9×10^{-5}	1.0	5.4×10^{-21}	1.9×10^{-18}	4.3×10^{-16}	1.2×10^{-16}	6.0×10^{-18}	1.4×10^{-13}	1.2×10^{-19}
aqueous phase									
$\Delta G_{(aq)rel}^{*}$ [b]	2.3	0.0	23.0	18.6	16.3	17.3	na[c]	16.3	0.7
population	0.02	0.76	9.8×10^{-18}	1.9×10^{-14}	8.8×10^{-13}	1.7×10^{-13}	na[c]	7.9×10^{-13}	0.22

[a] Relative energies with respect to $\Delta G_{(g)}^{\circ}$ for **Gh2**. [b] Relative energies with respect to $\Delta G_{(aq)}^{*}$ for **Gh2**. [c] Data not available.

$$\Delta G_{(sol)}^{*}(HA) = \Delta G_{(sol)}^{R'}(HA) + \Delta E_{(dis)}(HA) \quad (10)$$

$$\Delta E_{(dis)}(A^-) = E_{(g)}^{\circ}(A_{R'}^-) - E_{(g)}^{\circ}(A_R^-) \quad (11)$$

$$\Delta E_{(dis)}(HA) = E_{(g)}^{\circ}(HA_{R'}) - E_{(g)}^{\circ}(HA_R) \quad (12)$$

$$\Delta G_{(sol)}^{R'}(A^-) = G_{(aq)}^{*}(A_{R'}^-) - G_{(g)}^{*}(A_{R'}^-) \quad (13)$$

$$\Delta G_{(sol)}^{R'}(HA) = G_{(aq)}^{*}(HA_{R'}) - G_{(g)}^{*}(HA_{R'}) \quad (14)$$

This approximation has been employed for computational reasons, as it avoids the calculation, often problematic, of the normal modes in solution. As a check of the validity of this approximation, the partition functions for the gas phase and solution phase optimized geometries of two cationic, two neutral, and two anionic species were evaluated. The mean absolute deviation in the calculated relative free energy, $\Delta\Delta G$, of the species was found to be 0.1–0.7 kcal/mol. Semiempirical modification of the cavity scaling factor to more accurately predict the experimental pK_a values should reduce the impact of the differences in the partition functions.

When the standard free energy of solvation is expressed in terms of the distortion energy and the solvation energy of the distorted geometry, $\Delta G_{(sol)} = \Delta E_{(dis)} + \Delta G_{(sol)}^{R'}$, eq 5.3 becomes

$$pK_a = \frac{1}{2.303RT}(G_{(g)}^{\circ}(A_R^-) + \Delta G_{(sol)}^{R'}(A^-) + \Delta E_{(dis)}^{\circ}(A^-) - G_{(g)}^{\circ}(HA_R) - \Delta E_{(dis)}^{\circ}(HA) - \Delta G_{(sol)}^{R'}(HA) - 270.29) \quad (15)$$

This equation is used to calculate the site-specific pK_a for each tautomer.

3. Results and Discussion:

Selection of the Model Cavity. As anticipated in the previous section, the critical issue for exploring a biological system characterized by several tautomers and equilibrium in solution is to create a model capable of reproducing the experimental pK_a values. In particular, as the pK_a values are logarithmic functions of the free energy, a very high accuracy (within 2 kcal/mol) is needed. As has been demonstrated by Goddard's group,[25,33] the computational level adopted in this work is satisfactory for reproducing the gas phase proton affinity of nucleobases. However, there is not currently a standard procedure using the polarizable continuum model (PCM) to predict the solution free energies of the nucleobases with the same accuracy.

The PCM parameter optimized for the test set of DNA nucleobases considered in this study (Scheme 2) is the electrostatic scaling factor (α), which is a real number that is used to increase or decrease the radii of each sphere centered on the atoms.[79] The UFF set of atomic radii (see Table 1 in ref 80), with default value of the scaling factor $\alpha = 1.0$ (Gaussian
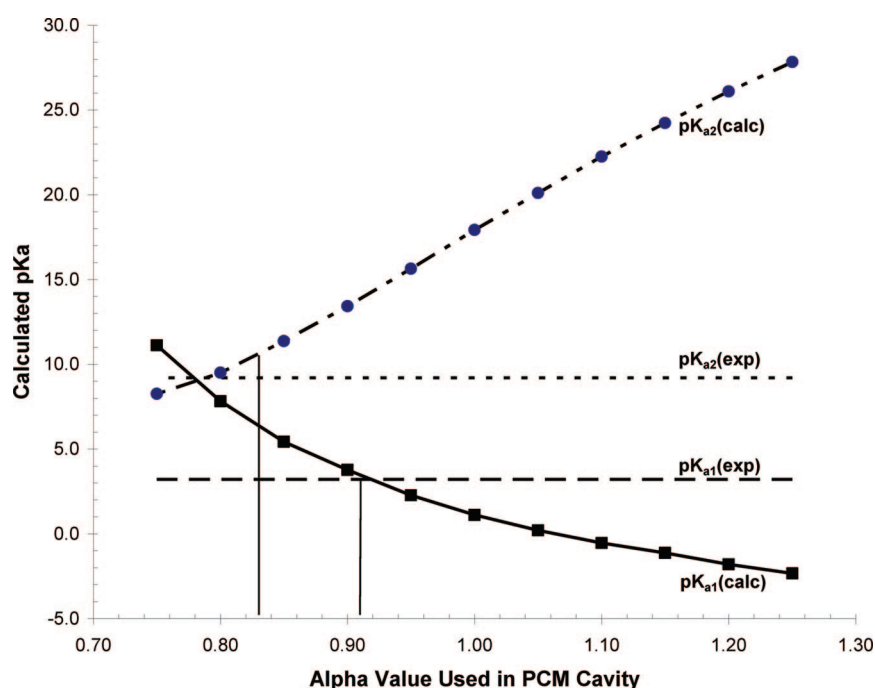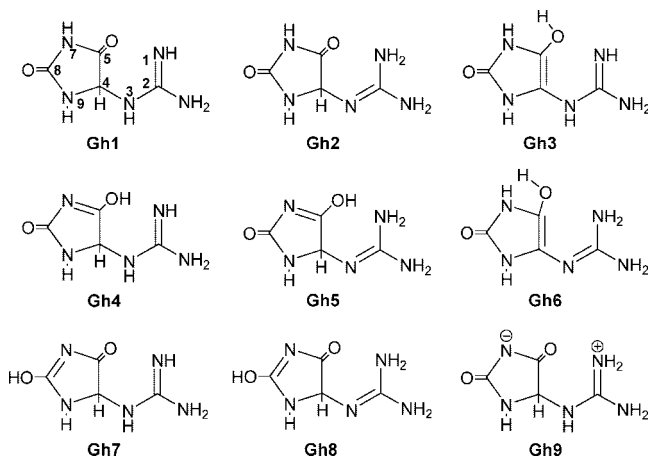

Figure 1. Effect of the UFF alpha value on the calculated pK_{a1} and pK_{a2} values of guanine.

pK_a Values of Nucleobases and Guanine Products

J. Phys. Chem. B, Vol. 112, No. 51, 2008 **16865**

SCHEME 3: Neutral Tautomers of Guanidinohydantoin Evaluated During This Study

Development Version E05), ensures a good balance between the computational stability and applicability and the reasonable accuracy of the free energy of solution for the neutral solutes.[79] For charged solutes, the scaling factor must be reconsidered. Due to the strong electrostatic interactions, solvent molecules are, in general, closest to the atoms of charged solutes rather than those of the neutral one.[85] In a recent study conducted by Camaioni's group, improved quantitative estimates of solvation effects in solution were obtained by decreasing the size of the cavity for cations and anions.[86] The representative nucleobase studied to set up the cavities used in this work was guanine, and various values of α were evaluated by comparing the calculated pK_a value with guanine's experimental first and second pK_a. Two different values of the scaling factor were adopted: to surround cationic and neutral intermediates a value of α = 0.91 showed the best results whereas, for anions, a smaller cavity with α = 0.83 has been used to provide good accuracy (Figure 1, Supporting Information Tables S12–S16).

Table 1 contains a summary of the relative free energy in the gas and solution phases, the free energy of solution, and the calculated and experimental values for the tautomers of guanine and the other nucleobases evaluated during this study. The calculated pK_a values and associated energy data for each deprotonation of the various guanine tautomers are provided in Supporting Information Scheme S1 and Table S1. On the basis of previous studies,[25] two cationic, two neutral, and three anionic tautomers were considered for the first and second guanine deprotonation (Scheme 2). In Table 1, the gas and solution phase energy for each tautomer is expressed relative to the most stable species of each class (e.g., guanine cations relative to the most stable guanine cation). The solvation free energy is also reported and clearly shows the effects of this contribution on the relative stability of the three anionic tautomers as the stability of **G5⁻** and **G6⁻** are reversed between the gas and solution phases. The two pK_a values computed are 3.4 and 9.6 for the first and the second deprotonation respectively, which are in good agreement with the experimental values of 3.2–3.3[33,87–93] and 9.2–9.6.[33,87–93]

Test of the Model Cavity on Other Nucleobases. To be sure that these new cavities could be extended to all the other nucleobases under study (Scheme 2), we have performed several test calculations on adenine, cytosine, thymine, and 8-oxoG and compared the predicted pK_a to the available experimental data. The data for the most abundant gas and solution phase tautomers are provided in Table 1. A complete summary of the data for all tautomers tested for adenine, cytosine, thymine, and 8-oxoG is provided in the Supporting Information Schemes S2–S5 and

Tables S2–S5. In the adenine system, the two most stable cationic tautomers are **A3⁺** (protonated at N1) and **A4⁺** (protonated at N3). In aqueous solution, the two most stable neutral tautomers are predicted to be **A6** and **A7**, which are similar in structure to the lowest energy guanine tautomers, **G3** and **G4**.

The global pK_a for adenine deprotonation has been estimated to be 4.2, in very good agreement with the experimental value of 4.1.[88,94] The calculations carried out on thymine show essentially only one neutral tautomer, the diketo **T1**, (Scheme 2) and two anions, **T2-** (deprotonation at N1) and **T3-** (deprotonation at N3), which are close in energy (Supporting Information Scheme S4 and Table S4) and predicted to be present at equilibrium in aqueous solution. All the other enol tautomers are predicted to be either completely absent or at such a low level as to not be relevant to the global pK_a calculation. In this case, the calculated pK_a was 10.5, which is in good agreement with the experimental value of 9.9.[88,94] Cytosine is a similar system to the pyrimidine base, thymine, but the presence of an amine functional group rather than a carbonyl group at C4 implies the potential existence of several enol imine tautomers (Supporting Information, Scheme S3 and Table S3). For cytosine, just one cationic and one neutral tautomer are predicted to be relevant in aqueous solution (i.e., **C1⁺** and **C2**, Table 1). Again a good agreement between calculated (4.2) and experimental pK_a (4.4) values has been found. Finally, in the 8-oxoG system, the data indicate that the presence of the carbonyl group at C8, instead of −CH, provides a drastic increase of acidity in N3, moving from 2.9 (local pK_a in guanine, see Supporting Information Scheme S1) to −0.4 (local and global first pK_a in 8-oxoG). This is in good agreement with the value found experimentally (∼0.1). Two different energies contribute to this value: the first one is a large difference between the gas phase basicity, which is calculated to be 218.3 kcal/mol for **G2⁺** → **G4** and 202.8 kcal/mol for **8-oxoG1⁺** → **8-oxoG2**. These calculations compare favorably with those of Goddard's group,[25,33] which predicted values of 216.18 and 200.8 kcal/mol for the same reactions, respectively, at B3LYP/6−31++G(d,p)//B3LYP/6−31G(d,p). The experimental value for the gas phase basicity of guanine is 222 ± 2 kcal/mol.[95] This energy gap is in part reduced by the contribution of polarization, and this is very clear if we consider the solvation free energies of the cationic and neutral intermediates of these two systems. As reported in Table 1 for guanine and 8-oxoG, the solvation energies of the neutral tautomers are comparable (−18.5 to −19.0 kcal/mol for guanine versus −21.0 kcal/mol for 8-oxoG) despite the presence of a more polar group in C8 of the 8-oxoG. In contrast, when the molecule is charged (i.e., cationic tautomers), the free energy of solvation for 8-oxoG is approximately 14−18 kcal/mol greater than for guanine, the energy gap between the 8-oxoG neutral and cationic species decreases, leading to a pK_a value near to −0.4. The second deprotonation of 8-oxoG involves two anionic tautomers, and also in this case, the calculated pK_a (8.00 units) is close to the experimental value (8.5−8.6[96]).

Summary of the Computational Method. Upon the basis of the good agreement between the predicted and experimental pKa values for the five nucleobases, the following steps were taken to calculate the pKa values for Gh and Sp:

(1) The geometry of each tautomer was optimized at B3LYP/6−31+G(d,p) and the frequencies were calculated.

(2) A gas phase single-point calculation was conducted on the gas phase optimized geometry (from Step 1) at B3LYP/aug-cc-pVTZ.

SCHEME 4: Structure and pK_a of Guanidine, Formylguanidine, Acetylguanidine, Hydantoin, and Phenytoin
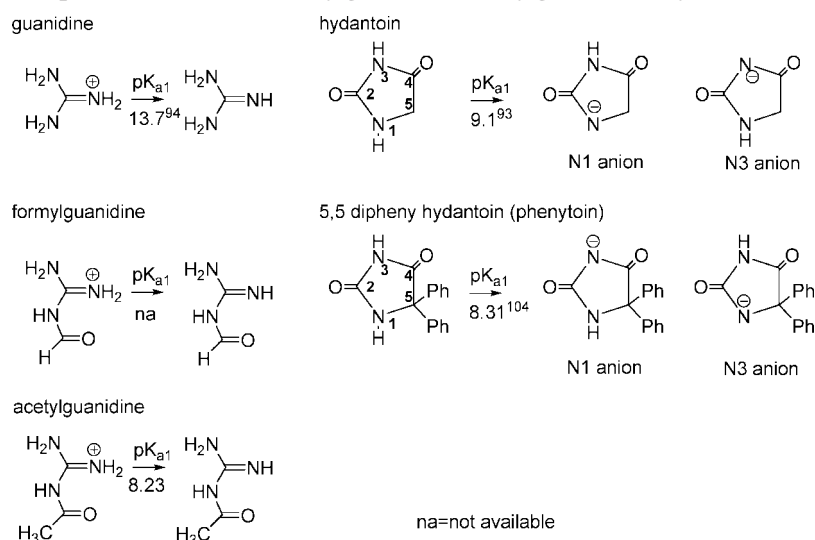
SCHEME 5: Cationic Tautomers of Gh Evaluated During This Study
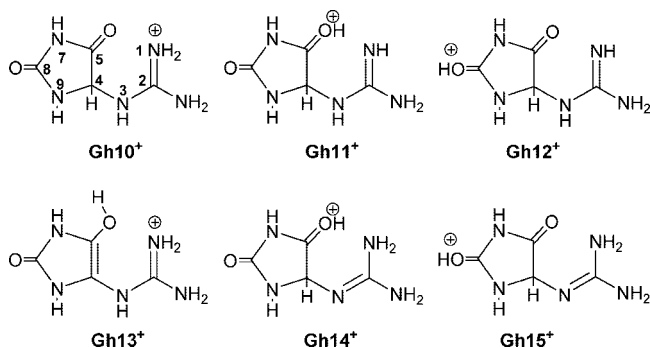
(3) The geometry of each tautomer was optimized in aqueous solution at IEF-PCM/B3LYP/6−31+G(d,p) using the gas phase optimized geometry as a starting point. The alpha value for this optimization was the default value of 1.00.

(4) A gas phase single point calculation was conducted on the aqueous phase optimized geometry (from Step 3) at B3LYP/aug-cc-pVTZ.

(5) The free energy of solvation for the solution phase optimized geometry (from Step 3) was obtained via a single-point calculation at IEF-PCM/B3LYP/6−31+G(d,p) using alpha values of 0.91 for the neutral and cationic tautomers and 0.83 for the anions.

(6) The free energy in solution of each tautomer and the site-specific or local pKa values are calculated using eqs 14 and 15, respectively.

Guanidinohydantoin Results. Several tautomers are possible for Gh for each ionization state and each is expected to contribute to an experimentally observable pK_a in proportion to its population in solution at 298 K. The free energies in the gas and aqueous phases of each of tautomer were calculated using the method described previously and are provided in Supporting Information Tables S8 and S9. The relative population of each species at 298 K was estimated assuming that the tautomers follow the Boltzmann distribution.

Tautomers of Neutral Guanidinohydantoin. The nine tautomers of neutral Gh considered in this study are shown in Scheme 3, and their relative free energies and populations in the gas and aqueous phases are given in Table 2. The gas phase electronic energies, sum of the zero point energy and thermal

corrections, and free energies of solvation for each species are provided in the Supporting Information Table S7. In the gas phase, the free energy of the neutral tautomers increases in the following order: **Gh2 < Gh1 ≪ Gh8 < Gh5 < Gh6 < Gh7 < Gh4 < Gh9 < Gh3**. The diketo forms of Gh (**Gh1**, **Gh2**, and **Gh9**) are 15−26 kcal/mol more stable than the enol tautomers (**Gh3−Gh8**). This result for the diketo forms of Gh are consistent with NMR, IR, UV, and dipole moment experimental data for hydantoin (Scheme 4), which demonstrated that the diketo species is predominant.[97−101] Earlier semiempirical calculations on hydantoin performed by Kleinpeter et al.[97] estimated that the diketo tautomer was 13−21.7 kcal/mol (PM3) and 15.6−25.2 kcal/mol (AM1) more stable the various imine enol species. **Gh2**, the N3−C2 imine tautomer, is the most stable species and is 6.4 kcal/mol lower in energy than **Gh1**, the C2−N1 imine species, due at least in part to the formation of a hydrogen bond between the terminal amino group and the oxygen of the C5 carbonyl group. Upon the basis of the calculated free energies, the gas phase equilibrium of Gh would consist almost exclusively of the **Gh2** tautomer.

In aqueous solution, the free energy of tautomers of neutral Gh increase in a slightly different order from that observed in the gas phase: **Gh2 ≈ Gh9 < Gh1 ≪ Gh8 < Gh5 < Gh6 < Gh7 < Gh4 < Gh3**. These data also indicate that the diketo tautomers—**Gh1**, **Gh2**, and **Gh9**—are more stable then the enol tautomers by 14−23 kcal/mol. Of the diketo tautomers, **Gh2** is predicted to be the most stable species followed by **Gh9** (+0.7 kcal/mol), a zwitterion formed by movement of a proton from N7 to N1, and **Gh1** (+2.3 kcal/mol). The stability of the zwitterion tautomer containing a protonated guanidine subunit (−N(H)C(NH$_2$)$_2$) is consistent with the experimentally observed basicity of guanidine (pK_a = 13.7)[102] and acidity of hydantoin (pK_a = 9.16) (Scheme 4).[103] The equilibrium in aqueous solution is predicted to consist of 76% **Gh2**, 22% **Gh9**, and 2% **Gh1**.

Tautomers of Cationic Guanidinohydantoin. Tautomers of cationic Gh considered in this study are shown in Scheme 5, and their relative free energies and populations in the gas and aqueous phases are given in Table 3. The N1 site appears to be the major site for protonation in both the gas and solution phases as the data suggest that the equilibrium concentration will consist almost entirely of the **Gh10$^+$** tautomer, the diketo hydantoin protonated at N1 of the guanidinyl subunit. This result is consistent with the known acidity and basicity of hydantoin and

TABLE 3: Relative Free Energies (kcal/mol) and Population of Cationic Tautomers of Gh

	Gh10+	Gh11+	Gh12+	Gh13+	Gh14+	Gh15+
Gas Phase						
$\Delta G^{\circ}_{(g)rel}$	0.0	47.8	41.4	23.0	32.1	25.0
population	1.0	3.7×10^{-29}	1.9×10^{-24}	5.5×10^{-11}	5.5×10^{-11}	2.0×10^{-12}
Aqueous Phase						
$\Delta G^{*}_{(aq)rel}$	0.0	36.2	32.2	20.2	35.5	27.7
population	1.0	2.8×10^{-27}	2.3×10^{-24}	1.5×10^{-15}	9.3×10^{-27}	4.9×10^{-21}

[a] Relative energies with respect to $\Delta G^{\circ}_{(g)}$ for **Gh10+**. [b] Relative energies with respect to $\Delta G^{*}_{(aq)}$ for **Gh10+**.

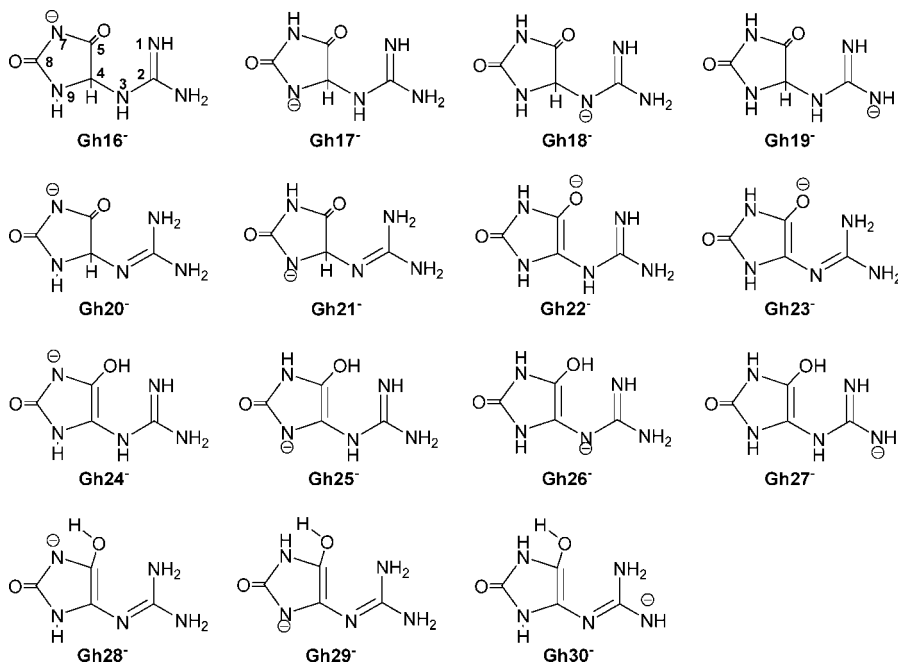**SCHEME 6: Anionic Tautomers of Gh Evaluated During This Study**

TABLE 4: Relative Free Energies (kcal/mol) and Population of Anion Tautomers of Gh

	Gh16−	Gh17−	Gh18−	Gh19−	Gh20−	Gh21−	Gh22−	Gh23−
Gas Phase[a]								
$\Delta G^{\circ}_{(g)rel}$	0.0	6.4	10.8	26.0	2.2	9.8	19.3	11.3
population	0.98	1.9×10^{-5}	1.1×10^{-8}	8.9×10^{-20}	0.02	6.3×10^{-8}	7.3×10^{-15}	5.4×10^{-9}
Aqueous Phase[b]								
$\Delta G^{*}_{(aq)rel}$	0.9	6.6	14.1	17.7	0.0	8.4	16.0	13.0
population	0.18	1.2×10^{-5}	3.8×10^{-11}	8.1×10^{-14}	0.82	5.6×10^{-7}	1.5×10^{-12}	2.3×10^{-10}

	Gh24−	Gh25−	Gh26−	Gh27−	Gh28−	Gh29−	Gh30−
Gas Phase[a]							
$\Delta G^{\circ}_{(g)rel}$	33.1	30.5	9.7	37.6	27.0	28.3	25.5[c]
population	5.0×10^{-25}	4.6×10^{-23}	8.2×10^{-8}	2.8×10^{-28}	1.6×10^{-20}	1.6×10^{-21}	2.1×10^{-19}
Aqueous Phase[b]							
$\Delta G^{*}_{(aq)rel}$	24.8	21.5	12.8	39.0	23.3	25.0	33.0
population	5.2×10^{-19}	1.4×10^{-16}	3.2×10^{-10}	2.1×10^{-29}	6.3×10^{-18}	3.7×10^{-19}	5.5×10^{-25}

[a] Relative energies with respect to $\Delta G^{\circ}_{(g)}$ for **Gh16−**. [b] Relative energies with respect to $\Delta G^{*}_{(aq)}$ for **Gh20−**. [c] The data shown are for the lowest energy rotamer of **Gh30−**. The relative free energy ranged from 25.5 to 36.0 kcal/mol and from 33.0 to 34.3 kcal/mol in the gas and aqueous phases, respectively.

guanidine. Similar to the pattern observed with the neutral tautomers, the **Gh10+** diketo form is significantly more stable than the enol tautomers **Gh13+**, **Gh14+**, and **Gh15+** in both the gas and solution phases. Protonation of the diketo form of Gh at either the C5 (**Gh11+**) or C8 (**Gh12+**) carbonyl oxygen results in a 23.0−47.8 kcal/mol increase in free energy in the gas phase and 20.2−36.2 kcal/mol increase in aqueous solution.

Tautomers of Anionic Guanidinohydantoin. Tautomers of anionic Gh considered in this study are shown in Scheme 6,

and their relative free energies and populations in the gas and aqueous phases are given in Table 4. The data indicate that deprotonation at the N7H imide position of the Gh diketone tautomers is energetically favored over all other sites as these tautomers, **Gh16−** and **Gh20−**, are at least 4 kcal/mol lower in energy than the next most stable species, **Gh17−**, a diketo N9 anion. These results are consistent with NMR data published by Kleinpeter[97] for a series of 5,5-disubstituted hydantoins demonstrating that the N3H imide proton (Scheme 4) located
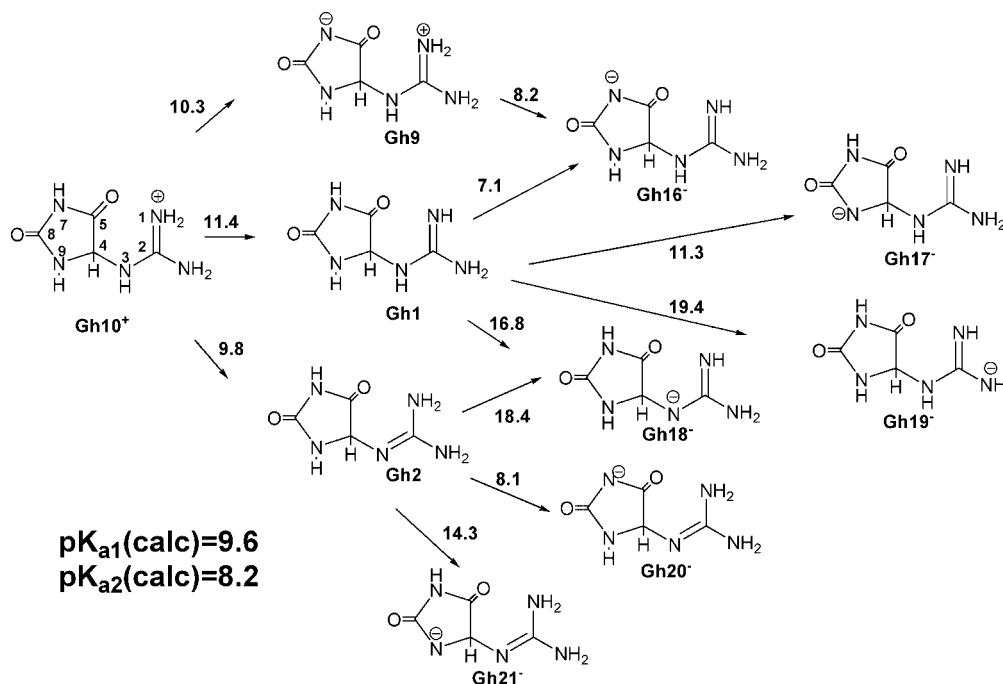
SCHEME 7: Local and Global pK$_a$ of Major Tautomers of Gh Evaluated During This Study

$$pK_{a1}(calc) = 9.6$$
$$pK_{a2}(calc) = 8.2$$

TABLE 5: Relative Free Energies (kcal/mol) and Population of Neutral Tautomers of Sp

	Sp1	Sp2	Sp3	Sp4	Sp5	Sp6	Sp7	Sp8
Gas Phase[a]								
$\Delta G^{\circ}_{(g)rel}$	0.0	1.4	1.3	2.0	19.5	19.7	19.7	12.2
population	0.81	0.08	0.08	0.03	4.1×10^{-15}	3.0×10^{-15}	2.8×10^{-15}	8.6×10^{-10}
Aqueous Phase[b]								
$\Delta G^{*}_{(aq)rel}$	0.0	3.7	6.8	7.0	19.9	19.7	22.1	19.1
population	1.0	1.8×10^{-3}	1.1×10^{-5}	7.0×10^{-6}	2.6×10^{-15}	3.6×10^{-15}	6.8×10^{-17}	1.1×10^{-14}

	Sp9	Sp10	Sp11	Sp12	Sp13	Sp14	Sp15
Gas Phase[a]							
$\Delta G^{\circ}_{(g)rel}$	19.9	20.3	18.2	20.0	19.5	19.3	15.6
population	2.1×10^{-15}	1.1×10^{-15}	3.7×10^{-14}	1.8×10^{-15}	3.9×10^{-15}	6.0×10^{-15}	3.2×10^{-12}
Aqueous Phase[b]							
$\Delta G^{*}_{(aq)rel}$	16.2	15.9	17.5	23.1	22.9	24.2	22.1
population	1.3×10^{-12}	2.1×10^{-12}	1.4×10^{-13}	1.2×10^{-18}	1.7×10^{-17}	1.8×10^{-18}	6.3×10^{-17}

[a] Relative energies with respect to $\Delta G^{\circ}_{(g)}$ for **Sp1**. [b] Relative energies with respect to $\Delta G^{*}_{(aq)}$ for **Sp1**.

between the two carbonyl groups was more acidic than the N1H amide proton. Similar to the data for the other Gh ionization states, the enol anions are much higher in energy than the diketo tautomers. As a consequence, in the gas phase, the population of anionic Gh is predicted to be 98% **Gh16$^-$** and 2% **Gh20$^{-\cdot}$**. In aqueous solution, the N3–C2 imine species, **Gh20$^-$**, is 0.9 kcal/mol more stable than **Gh16$^-$** and the population ratio is predicted to shift to 18% **Gh16$^-$** and 82% **Gh20$^-$**.

pK$_a$ of Guanidinohydantoin. Site-specific pK$_a$ values (pK_a^{ij}) for deprotonation of the various cationic and neutral tautomers of Gh were calculated from the change in free energy for each of the identified reactions using eqs 13–15 and are provided in Supporting Information Table S9. The global pK$_a$ of Gh was calculated using the Boltzmann weighting method outlined by Goddard[25,33] (eq 1) and assumes rapid equilibrium between the various tautomers in aqueous solution. The calculated values for site-specific and global deprotonation of the major tautomers of Gh are summarized in Scheme 7. The predicted pK$_{a1}$ value suggests that deprotonation of the Gh cation will likely occur at a pH of 9.6 at either the N3 position to form **Gh2** or at the imide (N7) position to form the **Gh9** zwitterionic tautomer. Once

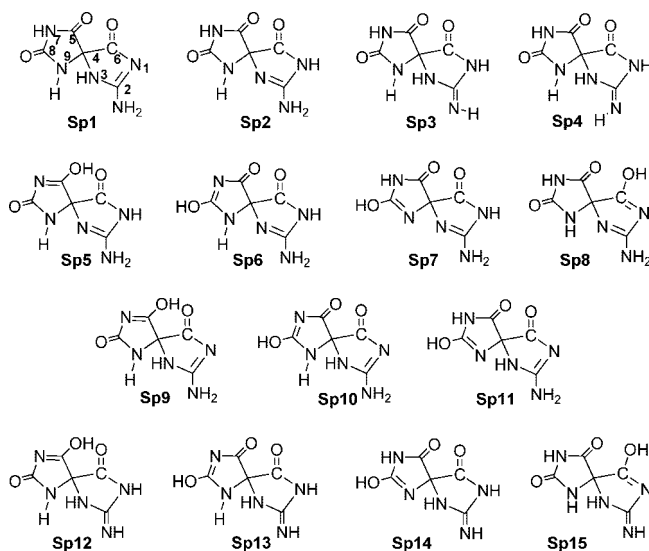**SCHEME 8: Neutral Tautomers of Sp Evaluated During This Study**

pKa Values of Nucleobases and Guanine Products

J. Phys. Chem. B, Vol. 112, No. 51, 2008 **16869**

TABLE 6: Relative Free Energies (kcal/mol) and Population of Cationic Tautomers of Sp

	Sp16$^+$	Sp17$^+$	Sp18$^+$	Sp19$^+$
Gas Phase^a				
$\Delta G^\circ_{(g)rel}$	0.0	21.1	15.7	26.6
population	1.0	3.7×10^{-16}	3.0×10^{-12}	3.0×10^{-20}
Aqueous Phase^b				
$\Delta G^*_{(aq)rel}$	0.0	na^c	22.3	26.0
population	1.0	na^c	4.3×10^{-17}	8.2×10^{-20}

na = not available. ^{a} Relative energies with respect to $\Delta G^\circ_{(g)}$ for **Sp16$^+$**. ^{b} Relative energies with respect to $\Delta G^*_{(aq)}$ for **Sp16$^+$**. ^{c} Data not available.

SCHEME 9: Cationic Tautomers of Sp Evaluated During This Study
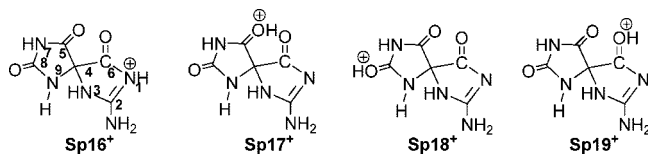
formed, the calculated pK_{a2} of 8.2 indicates that these neutral species should almost immediately undergo a second deprotonation to form the two N7 anion species, **Gh16$^-$** and **Gh20$^-$**. The data suggests that Gh will behave in a similar manner to its two subunits: guanidine (pK_a = 13.7) and hydantoin (pK_a = 9.16) but is slightly more acidic than either moiety alone. Using the same computational method discussed previously, the calculated pK_a values for guanidine and hydantoin are predicted to be 14.5 and 11.0, respectively. The increase in acidity of Gh is not unexpected given that some substituted guanidines and hydantoins demonstrate similar behavior. The experimental pK_a values for acetylguanidine and 5,5 diphenylhydantoin (phenytoin) are 8.32 and 8.31, respectively. The method described in this study predicts values of 8.5 for acetyl guanidine and 8.7 for phenytoin (Table 1, Supporting Information Scheme S7 and Tables S6 and S7). Experimental values for Gh have not been published to date; however, our results are consistent with SciFinder Scholar's online database for Gh, which lists empirically predicted pK_{a1} and pK_{a2} values of 15.83 ± 0.40 and 12.17 ± 0.70 (calculated using Advanced Chemistry Development software V8.14.).[104] Using the same software, the predicted values for guanidine and hydantoin are 13.27 ± 0.70 and 8.7 ± 0.50, respectively.

Neutral Tautomers of Spiroiminodihydantoin. The relative free energies and populations in the gas and aqueous phases of the various neutral tautomers of Sp considered in this study are given in Table 5 and in Tables S10 and S11 of the Supporting Information; their structures are provided in Scheme 8.

In the gas phase, the free energy of each neutral species increases in the following order: **Sp1** < **Sp3** ≈ **Sp2** < **Sp4** ≪ **Sp8** < **Sp15** < **Sp11** < **Sp14** < **Sp5, Sp13** < **Sp6, Sp7** < **Sp9** < **Sp12** < **Sp14**. Of the 15 tautomers, the 4 triketo species — **Sp1–Sp4** — are estimated to be the most stable species with a free energy difference between them of 2 kcal/mol. The remaining 11 tautomers are imine enol species and are at least 10−18 kcal/mol higher in energy than **Sp1–Sp4**, making their population negligible. In the gas phase, the equilibrium concentration is predicted to be 81% **Sp1** (the C2−N1 imine), 8% **Sp2** (the N3−C2 imine), 8% **Sp3** (a C2−N10 imine), and 3% **Sp4** (a rotamer of **Sp3**).

In aqueous solution, the free energy of the tautomers increases in a slightly different order: **Sp1** < **Sp2** < **Sp3** ≈ **Sp4** ≪ **Sp10** ≈ **Sp9** < **Sp11** < **Sp8** < **Sp6** ≈ **Sp5** < **Sp7, Sp15** < **Sp13** <

Sp12 < **Sp14**. The imine enol species—**Sp5−Sp15**—are again predicted to be significantly less stable than the four triketo tautomers, **Sp1−Sp4**. These results are also consistent with the experimental and theoretical data for hydantoin, which indicates that the keto species is thermodynamically preferred over the enol tautomers.[97−101] In aqueous solution, the difference in energy between **Sp1**, the lowest energy species, and **Sp2**, **Sp3**, and **Sp4** is 3.7, 6.8, and 7.0 kcal/mol, respectively. Therefore, at equilibrium, an aqueous solution of Sp will almost exclusively consist of the **Sp1** C2−N1 imine tautomer.

Cationic Tautomers of Spiroiminodihydantoin. Protonation of Sp can occur at the N1 position and on the oxygen of the carbonyl groups at C5, C6, or C8. The relative free energies and populations in the gas and aqueous phases of the four cationic tautomers of Sp considered in this study are given in Table 6; their structures are provided in Scheme 9. Both the gas and solution phase data indicate that **Sp16$^+$** is approximately 15−26 kcal/mol lower in energy than the other three cations, suggesting that Sp is almost exclusively protonated at a guanidinyl nitrogen rather than at one of the carbonyl oxygens.

Anionic Tautomers of Spiroiminodihydantoin. Depending on the neutral triketo tautomer, deprotonation of Sp can occur at the N1, N3, N7, or N9 positions of the hydantoin rings or from the terminal amino group at C2. For the imine enol tautomers, deprotonation can also occur at the C5, C6, or C8 hydroxyl groups. The relative free energies and populations in the gas and aqueous phases of the 12 anion tautomers of Sp considered in this study are given in Table 7; their structures are provided in Scheme 10. In the gas phase, the most stable tautomers are **Sp23$^-$** (0.0 kcal/mol), **Sp22$^-$** (0.86 kcal/mol), **Sp26$^-$** (1.7 kcal/mol), and **Sp29$^-$** (3.3 kcal/mol). The free energy of the remaining anionic tautomers increases in the following order: **Sp20$^-$** < **Sp31$^-$** ≈ **Sp27$^-$** < **Sp30$^-$** < **Sp28$^-$** ≈ **Sp21$^-$** ≈ **Sp24$^-$** < **Sp25$^-$**. In equilibrium in the gas phase, the composition is predicted to comprise 77% **Sp23$^-$**, 18% **Sp22$^-$**, and 4% **Sp26$^-$**.

In aqueous solution, the data suggest that the equilibrium composition will consist almost exclusively of the **Sp20$^-$** N7 anion triketo tautomer. All other tautomers are at least 4.5 kcal/mol higher in energy and will therefore represent less than 0.05% of the equilibrium population.

pK_a of Spiroiminodihydantoin. Site specific pK_a values (pK_a^{ij}) for deprotonation of the various cationic and neutral tautomers of Sp were calculated from the change in free energy for each of the identified reactions using eqs 13–15 and are provided in Supporting Information Table S10. The global pK_a of Sp was calculated using the Boltzmann weighting method discussed previously (eq 1). The calculated values for site-specific and global deprotonation of the major tautomers of Sp are summarized in Scheme 11. The predicted pK_{a1} value suggests that deprotonation of the Sp cation will likely occur at a pH of 0.5 and will most likely result from a loss of a proton at the N1 position. This calculated value is in line with both the experimentally observed (∼0.1) and calculated (−0.3) values for deprotonation of 8-oxoguanine.[23,25,33] Experimental data measuring the pK_a of Sp are not available; however, SciFinder Scholar's online database for Sp lists empirically predicted values of pK_{a1} = −0.19 and pK_{a2} = 7.79 (calculated using Advanced Chemistry Development software V8.14.).[104]

Once formed, the calculated pK_{a2} of 4.8 for deprotonation of neutral Sp indicates that this molecule is significantly more acidic than Gh (pK_{a2} = 8.2). A close review of the free energy data for the anion tautomers shows that the values for the global pK_{a2} of Sp and Gh are predominantly driven by deprotonation

16870 *J. Phys. Chem. B, Vol. 112, No. 51, 2008*

Verdolino et al.

TABLE 7: Relative Free Energies (kcal/mol) and Population of Anionic Tautomers of Sp

	Sp20⁻	Sp21⁻	Sp22⁻	Sp23⁻	Sp24⁻	Sp25⁻
Gas Phase[a]						
$\Delta G_{(g)rel}^{\circ}$	5.15	11.8	0.86	0.0	12.0	18.2
population	1.3×10^{-4}	1.6×10^{-9}	0.18	0.77	1.2×10^{-9}	3.3×10^{-14}
Aqueous Phase[b]						
$\Delta G_{(aq)rel}^{*}$	0.0	5.3	4.6	7.4	4.5	10.5
population	1.0	1.4×10^{-4}	4.0×10^{-4}	3.8×10^{-6}	4.7×10^{-4}	2.1×10^{-8}
	Sp26⁻	**Sp27⁻**	**Sp28⁻**	**Sp29⁻**	**Sp30⁻**	**Sp31⁻**
Gas Phase[a]						
$\Delta G_{(g)rel}^{\circ}$	1.7	6.9	11.6	3.3	8.5	6.4
population	0.04	7.2×10^{-6}	2.4×10^{-9}	2.9×10^{-3}	4.7×10^{-7}	1.5×10^{-5}
Aqueous Phase[b]						
$\Delta G_{(aq)rel}^{*}$	5.9	11.4	14.5	6.0	11.3	14.4
population	4.6×10^{-5}	4.5×10^{-9}	2.2×10^{-11}	3.9×10^{-5}	5.5×10^{-9}	2.8×10^{-11}

[a] Relative energies with respect to $\Delta G_{(g)}^{\circ}$ for **Sp23⁻**. [b] Relative energies with respect to $\Delta G_{(aq)}^{*}$ for **Sp20⁻**.

SCHEME 10: Anionic Tautomers of Sp Evaluated During This Study
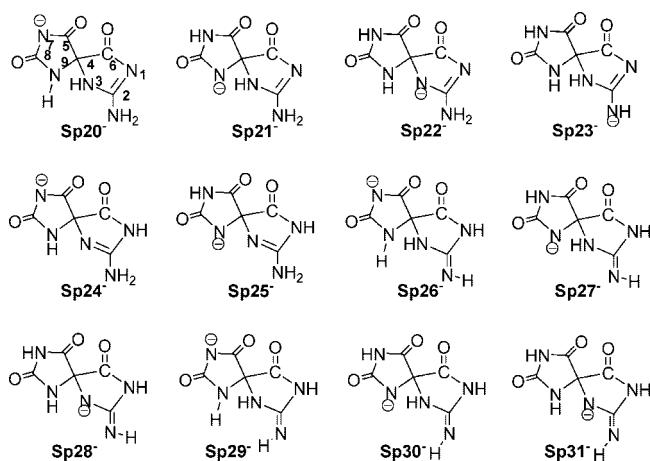
at the N7 position of each molecule. These results are consistent with NMR data indicating that the imide proton in both unmodified and 5,5-disubstituted hydantoins (i.e., the N3H proton, Scheme 4) is also the most acidic ring proton.[97] For Sp, based upon the Boltzmann weighting, the global pK_{a2} is almost exclusively represented by the deprotonation of **Sp1** at N7 leading to formation of **Sp20⁻**. For Gh, three reactions contribute to the global pK_{a2}: **Gh1** → **Gh16⁻** (pK_a = 7.1), **Gh2** → **Gh20⁻** (pK_a = 8.1); and **Gh9** → **Gh16⁻** (pK_a = 8.2). The first two reactions are deprotonations at the N7 position; the third is a deprotonation from N1 of the guanidinyl subunit of the zwitterion.

The predicted pK_a value of 4.8 for Sp seems surprisingly low for a substituted hydantoin; however, experimental data indicates that the pK_a of hydantoins is very much affected by substituents at N1 and C5 of the ring.[97] The experimentally measured pK_a of 5,5-diphenyl hydantoin, sold commercially as phenytoin, is 8.31, almost one full unit lower than the unmodified moiety.[105,106] The predicted value for phenytoin using the method described in this study, is 8.7 (Table 1). Modification of phenytoin at the N1 position to yield 1-phenylsulfonyl-5,5-diphenyl hydantoin, reduces the pK_a of the resulting substituted hydantoin to 4.89.[104,105]

In an effort to examine in detail, the factors contributing to the predicted difference in acidity between Sp and Gh, the contribution of each energy component of the calculation to the site specific pK_a was evaluated and is presented in Table 8.

Through-space substituent effects were also evaluated and are presented in the same table. Comparing the deprotonation of **Sp1** to **Gh2** (Gh N3 imine), the major neutral Gh tautomer, the difference in acidity is being driven by the gas phase free energy of the N7 anion relative to its neutral moiety. In the case of **Gh1** (C2N1 imine), and the zwitterion, **Gh9,** the difference in acidity is a consequence of the greater free energy of solvation associated with the Sp anion, **Sp20⁻**.

The hydantoin ring containing the N7 proton is the same structure for both Gh and Sp. One key difference between the two molecules is the presence of a carbonyl group located at the C6 position of Sp. The optimized geometry of Sp orients this carbonyl group directly over the hydantoin ring, and it is possible that the lone pair electrons of the oxygen are influencing the acidity of the imine proton (Figure 2). Through-space electronic effects[107] on the acidity of the imine (N7) and amine (N9) protons were evaluated by performing calculations on Sp by replacing the carbonyl at the C6 position with an ethylene group ($C=CH_2$) and a CH_2 group (Table 8). Deprotonation of four neutral tautomers of SpC6CH₂ at the N7 position was evaluated (Supporting Information Table S17 and S18). The predicted pK_a of Sp increases significantly as the electron-withdrawing nature of the substituent decreases with calculated values of 6.6 for **Sp(C6=CH₂)** and 11.9 for **Sp(C6H₂)**. Visual inspection of the predicted highest occupied molecular orbitals (HOMOs) for **Sp1**, **Sp(C6=CH₂)**, **Sp(C6H₂)** and **Gh1** (Figure 2) indicate that there is significant orbital overlap between the hydantoin ring of **Sp1** and the electrons of the C6 carbonyl group. This overlap is not observed for the other species. Through-space electronic effects of the lone-pair may therefore be partly responsible for the predicted increase in acidity of Sp vs Gh.

As indicated by the data in Table 7, the predicted relative population of Sp anions in the gas phase and in aqueous solution are significantly different. The difference is, in large part, the result of the approximately 10 kcal/mol larger free energy of solvation of the Sp N7 and N9 anions — **Sp20⁻**, **Sp21⁻**, **Sp24⁻**, and **Sp25⁻** — relative to the other anionic tautomers of Sp (Supporting Information Table S9). Careful review of the solvation data for these four N7 and N9 anionic tautomers indicates that they also have larger solution phase dipole moments (15.2−20.9 debye) relative to the other tautomers (4.6−13.7) due to the location of the anion and the lone pairs of the three carbonyl groups. It is possible that this large polarization of the solute cavity may result in an overestimation

SCHEME 11: Site-specific and global pK_a of major tautomers of Sp evaluated during this study

pK$_{a1}$ (calc) = 0.5
pK$_{a2}$ (calc) = 4.8
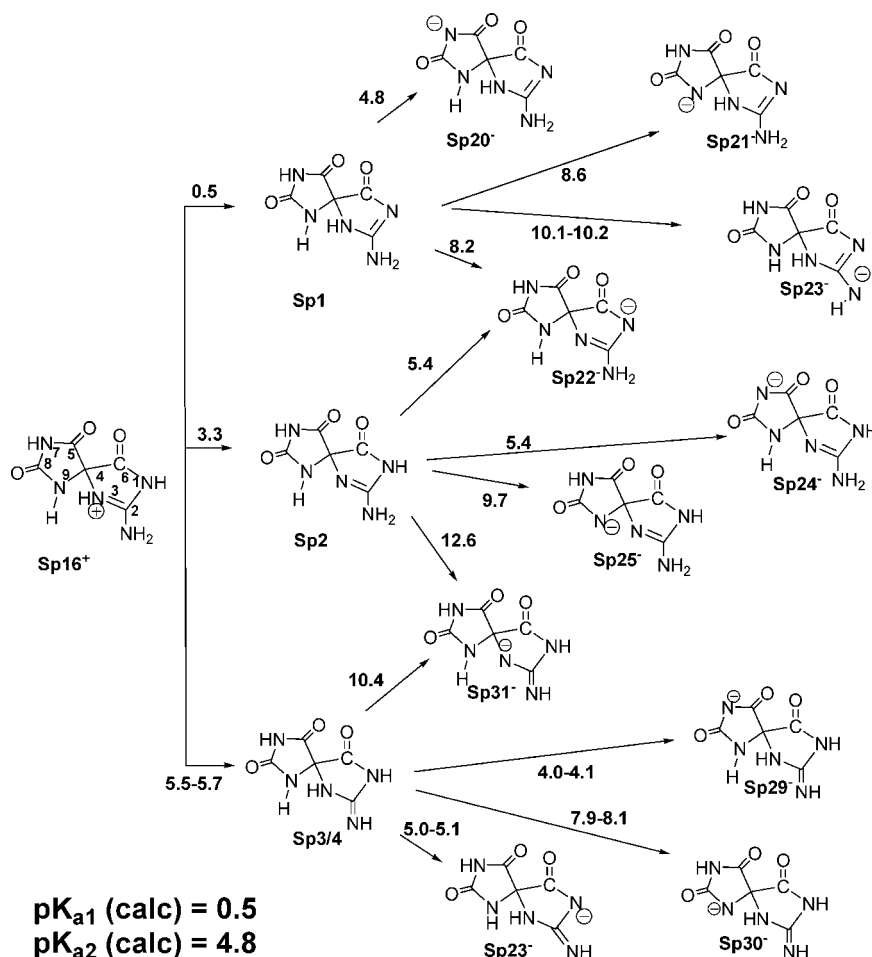
TABLE 8: Acidity of N7 Proton: Comparison of Sp1 with Sp1 (C6=CH$_2$), Sp (C6CH$_2$), Gh1, Gh2, and Gh9

Energy Components[a]	Sp1 (C6=O) (1.0)[b]	Sp1 (C6=CH$_2$)	Sp1 (C6H$_2$)
$\Delta G_{(g)}$	325.26	328.26	330.27
$\Delta\Delta G^{R'}_{(sol)}$	-56.90	-56.84	-51.37
$\Delta E_{(dis)}$	2.11	1.58	1.28
Site-Specific pK_a	**4.8**	**6.6**	**11.9**
Δ pK_a vs Sp5		*+1.8*	*+7.1*
diff G$_{(g)}$		+2.2	+3.7
diff G$_{(sol)}$		+0.0	+4.0
diff $\Delta E_{(dis)}$		-0.4	-0.6

Energy Components[a]	Gh1 (0.02)[b]	Gh2 (0.76)[b]	Gh9 (0.22)[b]
$\Delta G_{(g)}$	325.81	334.47	306.36
$\Delta\Delta G^{R'}_{(sol)}$	-54.30	-60.63	-29.7
$\Delta E_{(dis)}$	2.17	1.22	-1.43
Site-Specific pK_a	**7.1**	**8.1**	**8.2**
Δ pK_a vs Sp5	*+2.3*	*+3.3*	*+3.4*
diff G$_{(g)}$	+0.4	+6.7	-13.9
diff G$_{(sol)}$	+1.9	-2.7	+19.9
diff $\Delta E_{(dis)}$	+0.0	-0.7	-2.6

[a] All energies are expressed in kcal/mol and represent the change in energy resulting from deprotonation of the neutral molecule at N7. [b] Boltzmann weighting of neutral molecule.

of the free energy of solvation by the PCM model and a correspondingly low predicted pK_a value for this molecule. A similar effect was noted in the calculation of the pK_a of formylguanidine where a value of 6.7 was obtained. One of
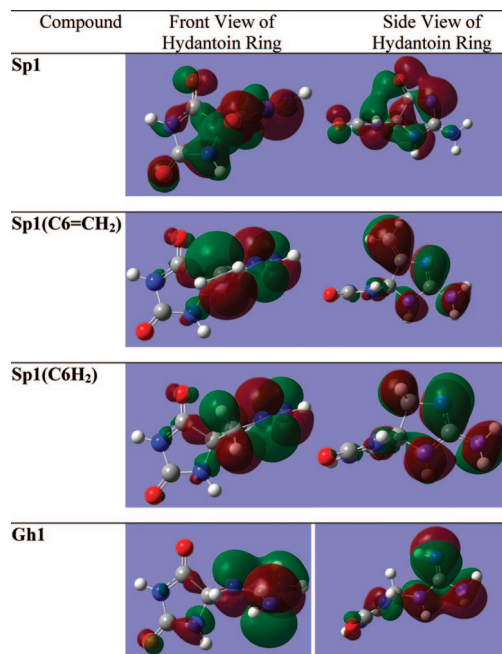
Figure 2. Comparison of HOMO molecular orbitals for **Sp1**, **Gh1**, **Sp1(C6=CH₂)** and **Sp1(C6H₂)**.

the tautomers, **FG8** (Supporting Information Scheme S6), had a calculated free energy of solvation nearly twice that of the other species and a local pK_a value of 5.0. No experimental value for N-formylguanidine was found in the literature; however, SciFinder Scholar's online database lists an empirically predicted value of $pK_{a1} = 7.75$ for this molecule (calculated using Advanced Chemistry Development software V8.14).[104]

Upon the basis of the analysis provided above, we believe that the observed pK_{a2} value for Sp is likely to be lower than that of Gh but higher than the 4.8 value predicted by the computational model described in this study. Calculations conducted with a methylene subtituent at the C6 carbon instead of a carbonyl group suggest that the pK_{a2} value for Sp may be in the range of 6.6–7.7 (Supporting Information Table S-18).

4. Conclusions

An efficient computational method has been identified that uses B3LYP density functional theory, IEF-PCM solvation modeling with a modified UFF cavity, and Boltzmann weighting of tautomers to predict the site-specific and global pK_a of DNA nucleobases and their oxidation products. The method is shown to be capable of predicting the global pK_a of the DNA nucleobases guanine, 8-oxoG, adenine, cytosine, and thymine to within 0.6 pK_a units of their experimental value. Predictions of the experimental values of phenytoin and N-acetylguanidine were within 0.4 pK_a units. The method works less-well for smaller molecules such as guanidine and hydantoin, where the calculated values are higher by 0.8 and 1.9 pK_a units, respectively.

The method has been used to evaluate the acidity of Gh and Sp, two highly mutagenic guanine oxidation products. The trend observed for the pK_a values of Gh (9.6 and 8.2) is consistent with the experimentally observed values for guanidine cation (13.7) and hydantoin (9.16). Molecular orbital predictions of the HOMO indicate that there is very little interaction between the hydantoin and guanidine subunits of Gh.

The pK_{a1}(calc) value for deprotonation of Sp cation (Sp⁺ → Sp) is very close to the experimentally observed pK_{a1} for 8-oxoG and is consistent with the similarity in their structures. The data

suggest that the imide (N7) proton in Sp may be more acidic than that in Gh, possibly due to the presence of the through-space electronic effects of the carbonyl group located at C6. This difference in the acidity of Gh and Sp may be an indication of their potential toxicity and mutagenicity in vivo and remains a fertile area for experimental study.

Supporting Information Available: Data used in the calculation of site-specific and global pK_as for the various species discussed in this manuscript are provided in the Supporting Information. The molecular geometries in Cartesian coordinates for the tautomers optimized in the gas phase are also provided. This material is available free of charge via the Internet at http://pubs.acs.org.

References and Notes

(1) Gimisis, T.; Cismas, C. *Eur. J. Org. Chem.* **2006**, 1351.
(2) Burrows, C. J.; Muller, J. G. *Chem. Rev.* **1998**, *98*, 1109.
(3) Breen, A. P.; Murphy, J. A. *Free Radical Biol. Med.* **1995**, *18*, 1033.
(4) Pratviel, G.; Meunier, B. *Chem.—Eur. J.* **2006**, *12*, 6018.
(5) Sayre, L. M.; Perry, G.; Smith, M. A. *Chem. Res. Toxicol.* **2008**, *21*, 172.
(6) Beckman, K. B.; Ames, B. N. *J. Biol. Chem.* **1997**, *272*, 19633.
(7) Foksinski, M.; Rozalski, R.; Guz, J.; Ruszkowska, B.; Sztukowska, P.; Piwowarski, M.; Klungland, A.; Olinski, R. *Free Radical Biol. Med.* **2004**, *37*, 1449.
(8) Steenken, S.; Jovanovic, S. V.; Bietti, M.; Bernhard, K. *J. Am. Chem. Soc.* **2000**, *122*, 2373.
(9) Luo, W. C.; Muller, J. G.; Rachlin, E. M.; Burrows, C. J. *Chem. Res. Toxicol.* **2001**, *14*, 927.
(10) Luo, W. C.; Muller, J. G.; Rachlin, E. M.; Burrows, C. J. *Org. Lett.* **2000**, *2*, 613.
(11) Niles, J. C.; Wishnok, J. S.; Tannenbaum, S. R. *Chem. Res. Toxicol.* **2004**, *17*, 1510.
(12) Ye, Y.; Muller, J. G.; Luo, W. C.; Mayne, C. L.; Shallop, A. J.; Jones, R. A.; Burrows, C. J. *J. Am. Chem. Soc.* **2003**, *125*, 13926.
(13) Suzuki, T.; Friesen, M. D.; Ohshima, H. *Chem. Res. Toxicol.* **2003**, *16*, 382.
(14) Munk, B. H.; Burrows, C. J.; Schlegel, H. B. *J. Am. Chem. Soc.* **2008**, *130*, 5245.
(15) *Principles of Biochemistry*, Fourth ed.; Lehninger, W. H. Ed.; Freeman and Company: New York, 2005.
(16) Chen, J. G.; McAllister, M. A.; Lee, J. K.; Houk, K. N. *J. Org. Chem.* **1998**, *63*, 4611.
(17) Acharya, P.; Cheruku, P.; Chatterjee, S.; Acharya, S.; Chatto-padhyaya, J. *J. Am. Chem. Soc.* **2004**, *126*, 2862.
(18) Acharya, S.; Barman, J.; Cheruku, P.; Chatterjee, S.; Acharya, P.; Isaksson, J.; Chattopadhyaya, J. *J. Am. Chem. Soc.* **2004**, *126*, 8674.
(19) Steenken, S.; Jovanovic, S. V. *J. Am. Chem. Soc.* **1997**, *119*, 617.
(20) Candeias, L. P.; Steenken, S. *J. Am. Chem. Soc.* **1989**, *111*, 1094.
(21) Roitzsch, M.; Lippert, B. *J. Am. Chem. Soc.* **2004**, *126*, 2421.
(22) Chatterjee, S.; Pathmasiri, W.; Plashkevych, O.; Honcharenko, D.; Varghese, O. P.; Maiti, M.; Chattopadhyaya, J. *Org. Biomol. Chem.* **2006**, *4*, 1675.
(23) Rogstad, K. N.; Jang, Y. H.; Sowers, L. C.; Goddard, W. A. *Chem. Res. Toxicol.* **2003**, *16*, 1455.
(24) Jang, Y. H.; Hwang, S. G.; Chung, D. S. *Chem. Lett.* **2007**, *36*, 1496.
(25) Jang, Y. H.; Goddard, W. A.; Noyes, K. T.; Sowers, L. C.; Hwang, S.; Chung, D. S. *J. Phys. Chem. B* **2003**, *107*, 344.
(26) Chandra, A. K.; Nguyen, M. T.; Zeegers-Huyskens, T. *J. Phys. Chem. A* **1998**, *102*, 6010.
(27) Chandra, A. K.; Michalska, D.; Wysokinsky, R.; Zeegers-Huyskens, T. *J. Phys. Chem. A* **2004**, *108*, 9593.
(28) Chandra, A. K.; Nguyen, M. T.; Uchimaru, T.; Zeegers-Huyskens, T. *J. Phys. Chem. A* **1999**, *103*, 8853.

(29) Chandra, A. K.; Nguyen, M. T.; Zeegers-Huyskens, T. *J. Mol. Struct.* **2000**, *519*, 1.

(30) Podolyan, Y.; Gorb, L.; Leszczynski, J. *J. Phys. Chem. A* **2000**, *104*, 7346.

(31) Giese, B.; McNaughton, D. *Phys. Chem. Chem. Phys.* **2002**, *4*, 5161.

(32) Tang, C. L.; Alexov, E.; Pyle, A. M.; Honig, B. *J. Mol. Biol.* **2007**, *366*, 1475.

(33) Jang, Y. H.; Goddard, W. A.; Noyes, K. T.; Sowers, L. C.; Hwang, S.; Chung, D. S. *Chem. Res. Toxicol.* **2002**, *15*, 1023.

(34) Kornyushyna, O.; Berges, A. M.; Muller, J. G.; Burrows, C. J. *Biochemistry* **2002**, *41*, 15304.

(35) Henderson, P. T.; Delaney, J. C.; Gu, F.; Tannenbaum, S. R.; Essigmann, J. M. *Biochemistry* **2002**, *41*, 914.

(36) Henderson, P. T.; Delaney, J. C.; Muller, J. G.; Neeley, W. L.; Tannenbaum, S. R.; Burrows, C. J.; Essigmann, J. M. *Biochemistry* **2003**, *42*, 9257.

(37) Duarte, V.; Muller, J. G.; Burrows, C. J. *Nucleic Acids Res.* **1999**, *27*, 496.

(38) Chinyengetere, F.; Jamieson, E. R. *Biochemistry* **2008**, *47*, 2584.

(39) Jia, L.; Shafirovich, V.; Shapiro, R.; Geacintov, N. E.; Broyde, S. *Biochemistry* **2005**, *44*, 13342.

(40) Jia, L.; Shafirovich, V.; Shapiro, R.; Geacintov, N. E.; Broyde, S. *Biochemistry* **2005**, *44*, 6043.

(41) Lim, C.; Bashford, D.; Karplus, M. *J. Phys. Chem.* **1991**, *95*, 5610.

(42) Hwang, S.; Jang, Y. H.; Chung, D. S. *Bull. Korean Chem. Soc.* **2005**, *26*, 585.

(43) Tissandier, M. D.; Cowen, K. A.; Feng, W. Y.; Gundlach, E.; Cohen, M. H.; Earhart, A. D.; Coe, J. V.; Tuttle, T. R. *J. Phys. Chem. A* **1998**, *102*, 7787.

(44) Sadlej-Sosnowska, N. *Theor. Chem. Acc.* **2007**, *118*, 281.

(45) Bryantsev, V. S.; Diallo, M. S.; Goddard, W. A. *J. Phys. Chem. A* **2007**, *111*, 4422.

(46) Burk, P.; Koppel, I. A.; Koppel, I.; Leito, I.; Travnikova, O. *Chem. Phys. Lett.* **2000**, *323*, 482.

(47) Barone, V.; Improta, R.; Rega, N. *Theor. Chem. Acc.* **2004**, *111*, 237.

(48) Farras, P.; Teixidor, F.; Branchadell, V. *Inorg. Chem.* **2006**, *45*, 7947.

(49) Ervin, K. M.; DeTuro, V. F. *J. Phys. Chem. A* **2002**, *106*, 9947.

(50) Kelly, C. P.; Cramer, C. J.; Truhlar, D. G. *J. Phys. Chem. A* **2006**, *110*, 2493.

(51) Liptak, M. D.; Gross, K. C.; Seybold, P. G.; Feldgus, S.; Shields, G. C. *J. Am. Chem. Soc.* **2002**, *124*, 6421.

(52) Liptak, M. D.; Shields, G. C. *Int. J. Quantum Chem.* **2001**, *85*, 727.

(53) Liptak, M. D.; Shields, G. C. *J. Am. Chem. Soc.* **2001**, *123*, 7314.

(54) Liptak, M. D.; Shields, G. C. *Int. J. Quantum Chem.* **2005**, *105*, 580.

(55) Merrill, G. N.; Kass, S. R. *J. Phys. Chem.* **1996**, *100*, 17465.

(56) Pliego, J. R. *Chem. Phys. Lett.* **2003**, *367*, 145.

(57) Pliego, J. R.; Riveros, J. M. *J. Phys. Chem. A* **2002**, *106*, 7434.

(58) Swart, M.; Bickelhaupt, F. M. *J. Chem. Theory Comput.* **2006**, *2*, 281.

(59) da Silva, C. O.; da Silva, E. C.; Nascimento, M. A. C. *J. Phys. Chem. A* **1999**, *103*, 11194.

(60) Silva, C. O.; da Silva, E. C.; Nascimento, M. A. C. *J. Phys. Chem. A* **2000**, *104*, 2402.

(61) Takano, Y.; Houk, K. N. *J. Chem. Theory Comput.* **2005**, *1*, 70.

(62) Saracino, G. A. A.; Improta, R.; Barone, V. *Chem. Phys. Lett.* **2003**, *373*, 411.

(63) Schuurmann, G.; Cossi, M.; Barone, V.; Tomasi, J. *J. Phys. Chem. A* **1998**, *102*, 6706.

(64) Hwang, S.; Jang, Y. H.; Cho, H.; Lee, Y. J. *Bull. Korean Chem. Soc.* **2008**, *29*, 539.

(65) Camaioni, D. M.; Schwerdtfeger, C. A. *J. Phys. Chem. A* **2005**, *109*, 10795.

(66) Frisch, M. J.; Trucks, G. W.; Schlegel, H. B.; Scuseria, G. E.; Robb, M. A.; Cheeseman, J. R.; Montgomery, J. A., Jr.; Vreven, T.; Scalmani, G.; Kudin, K. N.; Iyengar, S. S.; Tomasi, J.; Barone, V.; Mennucci, B.; Cossi, M.; Rega, N.; Petersson, G. A.; Nakatsuji, H.; Hada, M.; Ehara, M.; Toyota, K.; Fukuda, R.; Hasegawa, J.; Ishida, M.; Nakajima, T.; Honda, Y. ; Kitao, O.; Nakai, H.; Li, X.; Hratchian, H. P.; Peralta, J. E.; Izmaylov, A. F.; Brothers, E.; Staroverov, V.; Kobayashi, R.; Normand, J.; Burant, J. C.; Millam, J. M.; Klene, M.; Knox, J. E.; Cross, J. B.; Bakken, V.; Adamo, C.; Jaramillo, J.; Gomperts, R.; Stratmann, R. E.; Yazyev, O.; Austin, A. J.; Cammi, R.; Pomelli, C.; Ochterski, J. W.; Ayala, P. Y.; Morokuma, K.; Voth, G. A.; Salvador, P.; Dannenberg, J. J.; Zakrzewski, V. G.; Dapprich, S.; Daniels, A. D.; Strain, M. C.; Farkas, O.; Malick, D. K.; Rabuck, A. D.; Raghavachari, K.; Foresman, J. B.; Ortiz, J. V.; Cui, Q.; Baboul, A. G.; Clifford, S.; Cioslowski, J.; Stefanov, B. B.; Liu, G.; Liashenko, A.; Piskorz, P.; Komaromi, I.; Martin, R. L.; Fox, D. J.; Keith, T.; Al-Laham, M. A.; Peng, C. Y.; Nanayakkara, A.; Challacombe, M.; Chen, W.; Wong, M. W.; Pople, J. A. *Gaussian DV*, Revision E.05; Gaussian, Inc.: Wallingford, CT, 2006.

(67) Becke, A. D. *Phys. Rev. A* **1988**, *38*, 3098.

(68) Becke, A. *J. Chem. Phys.* **1993**, *98*, 5648.

(69) Lee, C.; Yang, W.; Parr, R. D. *Phys. Rev. B* **1988**, *37*, 785.

(70) Ditchfield, R.; Hehre, W. J.; Pople, J. A. *J. Chem. Phys.* **1971**, *54*, 724.

(71) Hehre, W. J.; Ditchfield, R.; Pople, J. A. *J. Chem. Phys.* **1972**, *56*, 2257.

(72) Hariharan, P. C.; Pople, J. A. *Theoret. Chim. Acta* **1973**, *28*, 213.

(73) Hariharan, P. C.; Pople, J. A. *Mol. Phys.* **1974**, *27*, 209.

(74) Gordon, M. S. *Chem. Phys. Lett.* **1980**, *76*, 163.

(75) Francl, M. M.; Pietro, W. J.; Hehre, W. J.; Binkley, J. S.; Gordon, M. S.; Defrees, D. J.; Pople, J. *Chem. Phys.* **1982**, *77*, 3654.

(76) Cances, E.; Mennucci, B.; Tomasi, J. *J. Chem. Phys.* **1997**, *107*, 3032.

(77) Cossi, M.; Barone, V.; Mennucci, B.; Tomasi, J. *Chem. Phys. Lett.* **1998**, *286*, 253.

(78) Mennucci, B.; Tomasi, J. *J. Chem. Phys.* **1997**, *106*, 5151.

(79) Tomasi, J.; Mennucci, B.; Cammi, R. *Chem. Rev.* **2005**, *105*, 2999.

(80) Rappe, A. K.; Casewit, C. J.; Colwell, K. S.; Goddard, W. A.; Skiff, W. M. *J. Am. Chem. Soc.* **1992**, *114*, 10024.

(81) Kendall, R. A.; Dunning, T. H.; Harrison, R. J. *J. Chem. Phys.* **1992**, *96*, 6796.

(82) Scott, A. P.; Radom, L. *J. Phys. Chem.* **1996**, *100*, 16502.

(83) McQuarrie, D. A. *Statistical Thermodynamics*; University Science Books: Mill Valley, CA, 1973.

(84) Ben-Naim, A.; Marcus, Y. *J. Chem. Phys.* **1984**, *81*, 2016.

(85) Orozco, M.; Luque, F. J. *Chem. Phys.* **1994**, *182*, 237.

(86) Ginovska, B.; Camaioni, D. M.; Dupuis, M. *J. Chem. Phys.* **2008**, 129.

(87) Lide, D. R. *CRC Handbook of Chemistry and Physics*, 80th ed.; CRC Press: Boca Raton, 1999−2000.

(88) Dawson, R. M. C.; Elliott, D. C.; Elliott, W. H.; Jones, K. M. *Data for Biochemical Research*, 3rd ed.; Oxford University Press: Oxford, 1986.

(89) Fasman, G. D. *CRC Handbook of Biochemistry and Molecular Biology, Nucleic Acids*, 3rd ed.; CRC Press: Cleveland, OH, 1975; Vol. 1.

(90) Ts'o, P. O. P. *Basic Principles in Nucleic Acid Chemistry*; Academic Press: New York, 1974.

(91) Jordan, D. O. *The Chemistry of Nucleic Acids*; Butterworth and Co.: WA, 1960.

(92) Chargaff, E., Davidson, J. N. *The Nucleic Acids Chemistry and Biology*; Academic Press: New York, 1955.

(93) Bundari, S. *The Merck Index*, 12th ed.; Merck and Company: Whitehouse Station, NJ, 1996.

(94) Shugar, D.; Fox, J. J. *Biochim. Biophys. Acta* **1952**, *9*, 199.

(95) Sowers, L. C.; Shaw, B. R.; Veigl, M. L.; Sedwick, W. D. *Mutat. Res.* **1987**, *177*, 201.

(96) Cho, B. P. *Magn. Reson. Chem.* **1993**, *31*, 1048.

(97) Kleinpeter, E.; Heydenreich, M.; Kalder, L.; Koch, A.; Henning, D.; Kempter, G.; Benassi, R.; Taddei, F. *J. Mol. Struct.* **1997**, *403*, 111.

(98) Kleinpeter, E. *Struct. Chem.* **1997**, *8*, 161.

(99) Cristiani, F.; Devillanova, F. A.; Diaz, A.; Isaia, F.; Verani, G. *Spectroc. Acta Pt. A—Molec. Biomolec. Spectr.* **1985**, *41*, 487.

(100) Sohar, P. *Acta Chim. Sci. Hung.* **1986**, *57*, 165.

(101) Sohar, P.; Nyitrai, J.; Zauer, K.; Lempert, K. *Acta Chim. Sci. Hung.* **1970**, *65*, 189.

(102) Albert, A.; Goldacre, R.; Phillips, J. *J. Chem. Soc.* **1948**, 2240.

(103) Bausch, M.; Selmarten, D.; Gostowski, R.; Dobrowolski, P. *J. Phys. Org. Chem.* **1991**, *4*, 67.

(104) *ACS SciFinder Scholar Registry;* American Chemical Society, 2008.

(105) de Oliveira, S. M.; da Silva, J. B. P.; Hernandes, M. Z.; de Lima, M. D. A.; Galdino, S. L.; Pitta, I. D. *Quim. Nova* **2008**, *31*, 614.

(106) Fujioka, H.; Tan, T. *J. Pharm. Bio-Dyn.* **1982**, *5*, 475.

(107) Anslyn, E. V.; Dougherty, D. A. *Modern Physical Organic Chemistry*; University Science Books: Sausalito, CA, 2006; Ch. 5.

(108) *Lange's Handbook of Chemistry*; 15th ed.; Dean, J. A. Ed.; McGraw Hill: Norwich, NY, 1999, pp 8−24.